2006

An Exonic Splicing Silencer Is Involved In The Regulated Splicing Of Glucose 6-Phosphate Dehydrogenase Mrna

Wioletta Szeszel-Fedorowicz

Indrani Talukdar

Brian N. Griffith

Callee M. Walsh

Lisa M. Salati

THE JOURNAL OF BIOLOGICAL CHEMISTRY VOL. 281, NO. 45, pp. 34146–34158, November 10, 2006

An Exonic Splicing Silencer Is Involved in the Regulated Splicing of Glucose 6-Phosphate Dehydrogenase mRNA*

Received for publication, April 20, 2006, and in revised form, September 14, 2006 Published, JBC Papers in Press, September 15, 2006, DOI 10.1074/jbc.M603825200

Wioletta Szeszel-Fedorowicz, Indrani Talukdar, Brian N. Griffith, Callee M. Walsh, and Lisa M. Salati[1]

From the Department of Biochemistry and Molecular Pharmacology, West Virginia University, Morgantown, West Virginia 26506

The inhibition of glucose-6-phosphate dehydrogenase (G6PD) expression by arachidonic acid occurs by changes in the rate of pre-mRNA splicing. Here, we have identified a cis-acting RNA element required for regulated splicing of G6PD mRNA. Using transfection of G6PD RNA reporter constructs into rat hepatocytes, the cis-acting RNA element involved in this regulation was localized to nucleotides 43–72 of exon 12 in the G6PD mRNA. In *in vitro* splicing assays, RNA substrates containing exon 12 were not spliced. In contrast, RNA substrates containing other regions (exons 8 and 9 or exons 10 and 11) of the G6PD mRNA were efficiently spliced. Furthermore, exon 12 can inhibit splicing when substituted for other exons in RNA substrates that are readily spliced. This activity of the exon 12 regulatory element suggests that it is an exonic splicing silencer. Consistent with its activity as a splicing silencer, spliceosome assembly was inhibited on RNA substrates containing exon 12 compared with RNAs representing other regions of the G6PD transcript. Elimination of nucleotides 43–72 of exon 12 did not restore splicing of exon 12-containing RNA; thus, the 30-nucleotide element may not be exclusively a silencer. The binding of heterogeneous nuclear ribonucleoproteins K, L, and A2/B1 from both HeLa and hepatocyte nuclear extracts to the element further supports its activity as a silencer. In addition, SR proteins bind to the element, consistent with the presence of enhancer activity within this sequence. Thus, an exonic splicing silencer is involved in the inhibition of splicing of a constitutively spliced exon in the G6PD mRNA.

Glucose-6-phosphate dehydrogenase (G6PD)[2] is a member of a family of enzymes that catalyze the *de novo* synthesis of fatty acids. In liver, the lipogenic pathway plays an essential role in converting excess dietary energy into a storage form. Consistent with this role in energy homeostasis, the capacity of this pathway is regulated by dietary changes, such as fasting, feeding, and the amount and type of carbohydrate and polyunsaturated fat in the diet (1). For many of the lipogenic enzymes, regulation of enzyme amount occurs primarily by changes in the transcription rate of the gene, but posttranscriptional regulation via mRNA stability has also been implicated (1). G6PD differs from the other family members in that dietary regulation occurs exclusively at a posttranscriptional step (2–4).

G6PD expression is inhibited by polyunsaturated fatty acids, such as arachidonic acid; this occurs at a unique posttranscriptional step involving a decrease in the rate of splicing of the nascent G6PD transcript. Several lines of evidence indicate that changes in mature mRNA accumulation are caused by changes in the efficiency of splicing of the G6PD transcript. First, changes in the cytoplasmic accumulation of G6PD mRNA are preceded by changes in the accumulation of mRNA in the nucleus in the absence of changes in transcriptional activity of the gene (3–5). Second, stimulatory treatments, such as refeeding, enhance the rate of accumulation of partially and fully spliced G6PD mRNA with little or no change in abundance of the primary transcript (2). Third, inhibition of G6PD expression by polyunsaturated fat results in an accumulation of partially spliced mRNA in the nucleus despite a decrease in the nuclear content of mature mRNA (6). Finally, using transient transfection of RNA reporter constructs containing progressive deletion of the 13 exons of the G6PD precursor mRNA (pre-mRNA) into rat hepatocytes, we have demonstrated that exon 12 and its surrounding introns are necessary for the arachidonic acid inhibition of mRNA accumulation (6). Thus, we conclude that G6PD expression is regulated by changes in the rate of pre-mRNA splicing.

This mechanism of regulation of G6PD by inhibition of its splicing may be shared across other metabolic genes, even those regulated by transcriptional mechanisms. In this regard, nutritional status regulates expression of the tricarboxylate (citrate) carrier and spot 14, a putative lipogenic protein by a nuclear posttranscriptional mechanism (2, 7–9). Regulation of accumulation of spliced intermediates has been observed for these genes, but the molecular details are not known. Regulating gene expression by changes in the rate of pre-mRNA splicing in addition to transcriptional regulation would result in a more rapid response to nutritional or hormonal changes.

Pre-mRNA splicing results in the removal of introns from primary transcripts and the joining of the exons containing the protein coding information. The G6PD gene is over 18

* This work was supported by National Institutes of Health Grant DK46897 (to L. M. S.), American Heart Association Grant 0315129B (to B. N. G.), the COBRE for Signal Transduction and Cancer (National Institutes of Health Grant P20RR016440), and the West Virginia University Proteomics Facility. The costs of publication of this article were defrayed in part by the payment of page charges. This article must therefore be hereby marked "*advertisement*" in accordance with 18 U.S.C. Section 1734 solely to indicate this fact.

[1] To whom correspondence should be addressed: Dept. of Biochemistry and Molecular Pharmacology, West Virginia University Health Sciences Center, P.O. Box 9142, Morgantown, WV 26506. Tel.: 304-293-7759; E-mail: Lsalati@hsc.wvu.edu.

[2] The abbreviations used are: G6PD, glucose-6-phosphate dehydrogenase; pre-mRNA, precursor-mRNA; ESE, exonic splicing enhancer; SR, serine/arginine-rich; snRNP, small nuclear ribonucleoprotein particle; hnRNP, heterogeneous nuclear ribonucleoprotein; ESS, exonic splicing silencer; CMV, cytomegalovirus; UTR, untranslated region; U2AF, U2 auxiliary factor; X_{corr}, cross-correlation; nt, nucleotide; LC, liquid chromatography; MS, mass spectrometry.

kb, and all of its exons are constitutively spliced. Exons can be constitutively or alternatively spliced. Constitutively spliced exons are those always present in the mRNA and account for the majority of exons. The alternative splicing of mRNA transcripts, which occurs for at least 60% of all genes, results in the production of different proteins and can occur in a tissue- or treatment-specific manner (10). Both constitutive and alternative splicing requires distinguishing exons from the surrounding intronic RNA. Exon definition, as the process of exon recognition is called, utilizes intronic sequences, which include the 5′ and 3′ splice sites, polypyrimidine tract, and branch point, as well as sequence elements in the exon called exonic splicing enhancers (ESEs) (11). ESEs are not highly conserved with respect to sequence and thus must be functionally characterized in the pre-mRNA (12, 13). The activity of ESEs involves their binding by members of a family of splicing regulatory proteins, serine/arginine-rich (SR) proteins (14). SR proteins participate in splicing by enhancing the recruitment of the key spliceosome components, U1 small nuclear ribonucleoprotein particle (snRNP) and U2 snRNP (11). In the absence of an ESE, binding of U1 and U2 snRNPs to the 5′ splice site and branch point, respectively, is less stable, and the rate of complex formation is slowed (11, 15).

Pre-mRNA splicing can also be inhibited by the action of silencer elements in the RNA. These sequences are present in both introns and exons and are bound by a diverse group of proteins that include some members of the heterogeneous nuclear ribonucleoprotein (hnRNP) family of proteins (16–19). Like enhancer elements, silencers exhibit great sequence diversity, and their identification in mRNA requires functional tests for their activity (19–21). When the silencer is present in the intron, it functions to suppress recognition of the splice sites; this is a key mechanism in alternative splicing (10). In contrast, exonic splicing silencers (ESSs) suppress exon definition, which involves interference with the binding of a splicing co-activator (22–24). In this regard, the juxtaposition of ESS and ESE elements in an exon results in the mutually exclusive binding of hnRNPs *versus* SR proteins (*cf.* Refs. 23 and 24). Although the role of ESSs in regulating splicing is best understood in alternative splicing, computational approaches suggest that ESSs are also present in constitutively spliced exons (21). The molecular details by which ESSs can regulate the splicing of constitutive exons remain largely unexplored.

G6PD mRNA is not alternatively spliced; thus, the regulation of its splicing by nutritional factors involves changes in the rate of splicing of a constitutively spliced exon. Understanding the molecular details by which G6PD pre-mRNA splicing is regulated will provide novel information on the mechanisms by which cells can regulate the rate of constitutive splicing and the role this process can play in controlling gene expression. In the present report, we identify the splicing regulatory element involved in the inhibition of G6PD pre-mRNA splicing by polyunsaturated fatty acids. This 30-nt regulatory element contains an ESS. The ESS can block the splicing of heterologous introns in an *in vitro* splicing assay. Consistent with its activity as a silencer, the exon 12 element inhibits spliceosome assembly by attenuating the formation of the first ATP-requiring complex in this process and binds hnRNPs, associated with inhibition of splicing. This is the first report of an ESS in a constitutively spliced exon being involved in the regulation of gene expression.

EXPERIMENTAL PROCEDURES

Animal Care and Cell Culture—Male Sprague-Dawley rats (175–250 g) were fed a chow diet and then starved 16 h prior to hepatocyte isolation. Hepatocytes were isolated by a modification of the Seglen technique (25) as described previously (4). Hepatocytes (3.1×10^6) were placed in 60-mm dishes coated with rat tail collagen and incubated in Hi/Wo/BA medium (Waymouth MB752/l plus 20 mM Hepes, pH 7.4, 0.5 mM serine, 0.5 mM alanine, 0.2% bovine serum albumin) plus 5% newborn calf serum (37 °C, 5% CO_2). Cell viability in all experiments was 90% or greater as estimated by trypan blue (0.04%) exclusion. After 3–4 h, the medium was replaced with serum-free medium, and the constructs presented in Figs. 1 and 2 were transfected. Each construct (2.5 μg/plate) was transfected using Lipofectin according to the manufacturer's protocol (Invitrogen). The ratio of DNA to liposome reagent was 1:6.7. A Matrigel overlay (0.3 mg/ml; BD Pharmingen) was added to hepatocytes 4 h after the transfection was begun (26). The transfection medium remained on the hepatocytes for 16 h and then was replaced with medium containing the treatments indicated in the figure legends. Subsequently, the medium was changed every 12 h to one of the same composition. Arachidonic acid (Nu-Check Prep, West Elysian, MN) was bound to bovine serum albumin (27). The fatty acid (4 mM)/albumin (1 mM) stock contained butylated hydroxytoluene (0.01%), and the medium contained α-tocopherol phosphate, disodium (10 μg/liter), to minimize oxidation of the fatty acids.

Construction of RNA Reporter Plasmids and Templates for the in Vitro Splicing Assay—Plasmids used in the analysis of cis-acting elements in the G6PD primary transcript were made using pGL3-Basic (Promega Corp.) as the vector backbone. The luciferase gene was removed from this vector, and portions of G6PD genomic DNA and the cytomegalovirus (CMV) promoter/enhancer sequences (1–640 bp from the pCMVβ vector; Clontech) were inserted into the multiple cloning site. Mutated RNA reporter constructs were prepared by replacing the G6PD sequence indicated in the legend to Fig. 2 with the sequence AAGCATGCAA using overlap extension PCR (28). The plasmid pβgal ex12-ex13 was made by replacing luciferase with the β-galactosidase gene from pCMVβ. G6PD sequences from nucleotide 37 of exon 12 through the end of the gene were ligated into β-galactosidase, deleting the terminal 13 amino acids of the β-galactosidase protein. The pβgal in12-ex13 plasmid deletes all but the last 8 nt of exon 12 to maintain the 5′-splice site. All sequences were evaluated to ensure that premature termination codons did not arise during cloning. Templates (Fig. 3*A*) for preparing *in vitro* splicing substrates were synthesized by PCR using either wild type G6PD sequences or the mutated sequences described above as templates. The T3 promoter was introduced by PCR upstream of the first exon in the substrate, and the PCR products were used in the *in vitro* transcription reactions. The templates for the chimeric splicing

substrates (Fig. 3*C*) were generated using overlap extension PCR and cloned downstream of a T7 promoter in pKS$^+$ (Stratagene). These plasmids were linearized with XbaI prior to *in vitro* transcription of the RNA. The template for the β-globin *in vitro* splicing substrate (pSP64-Hβδ6) was obtained from Dr. Adrian Krainer (29).

Isolation of Total RNA and Ribonuclease Protection Assay—Total RNA from three plates per treatment was isolated by the method of Chomczynski and Sacchi (30). Quantitation of transgene and endogenous mRNA was conducted using RNase protection assays (Ambion, Inc.) as previously described (6). β-Actin mRNA was used as a loading control. The template for rat β-actin was purchased from Ambion, Inc. The resulting hybridization products protected from RNase digestion were separated in a 6% (7 M urea) polyacrylamide gel. Images were visualized by storage phosphorimaging and quantified using ImageQuant software (Amersham Biosciences).

In Vitro Splicing Assay—In vitro splicing substrates were synthesized by *in vitro* transcription of the G6PD minigenes with T7 or T3 polymerase using [^{32}P]CTP. HeLa cell nuclear extract was purchased from Promega or prepared as previously described (31) with packed HeLa S3 cells from the National Cell Culture Center. Splicing assays were performed in 20-μl reaction volumes containing 10–20 ng of ^{32}P-labeled *in vitro* splicing substrate, 40% (v/v) nuclear extract, 20 mM Hepes, pH 7.4, 0.5 mM ATP, 20 mM creatine phosphate, 3 mM $MgCl_2$, and 2.5% polyvinyl alcohol. Reactions were incubated for 4 h unless otherwise stated in the figure legends. Reactions were stopped by the addition of 200 μl of stop-splicing solution (0.3 M sodium acetate, pH 5.2, 0.1% (w/v) SDS, 62.5 μg/ml tRNA) (32). RNA was purified from the splicing mixture with Tris-HCl-saturated phenol (pH 8.0) followed by precipitation with ethanol. Splicing products were analyzed on 6% denaturing polyacrylamide gels and visualized by storage phosphorimaging. Quantification of splicing reactions in Fig. 4*B* was performed as follows. Radioactive bands corresponding to the spliced products and unspliced *in vitro* splicing substrates were quantified with ImageQuant. These values were corrected with respect to the number of cytosines in each band and are referred to as normalized PhosphorImager units. The percentage of spliced mRNA was calculated as the ratio of the normalized PhosphorImager units of spliced mRNA divided by the sum of the amounts of unspliced plus spliced RNA. Statistical analysis of spliced product accumulation used one-way analysis of variance and least squares fit (33).

Spliceosome Assembly and Gel Electrophoresis—Analysis of spliceosome complex formation was conducted by incubating the RNA substrates in the splicing conditions described above. At the time points indicated in Fig. 5, heparin (0.2 mg/ml) was added to the splicing mixture. After incubation for an additional 5 min at 30 °C, the samples were placed on ice, and 5 μl of each reaction was fractionated on a native 4% polyacrylamide gel (acrylamide/bisacrylamide, 80:1), using 200 V at room temperature for 3 h (34). For agarose gel electrophoresis, *in vitro* splicing mixtures were incubated without heparin and were placed on ice at the indicated time points (Fig. 6). The complexes (5 μl of each reaction) were separated using electrophoresis in 1.5% low melting point agarose at 70 V for 3 h (35).

UV Cross-linking Assay—UV cross-linking was preformed as described (36). The reaction mixtures contained 5 μg of nuclear extract protein and 10–20 fmol of substrate RNA (50,000–100,000 cpm). Binding of proteins to the RNA was visualized using storage phosphorimaging and quantified using ImageQuant.

RNA Affinity Assay—RNA oligomers were covalently linked to adipic acid dihydrazide-agarose beads (37, 38). Briefly, 1000 pmol of RNA in a 400-μl reaction mixture containing 100 mM sodium acetate, pH 5.0, and 5 mM sodium *m*-periodate was incubated for 1 h in the dark at room temperature. The RNA was ethanol-precipitated and resuspended in 500 μl of 0.1 M sodium acetate, pH 5.0. Adipic acid dihydrazide-agarose beads (400 μl; Sigma) were washed four times in 10 ml of 0.1 M sodium acetate, pH 5.0, and then mixed with the periodate-treated RNA. The beads with the bound RNA were washed three times with 2 M NaCl and three times with 20 mM HEPES-KOH, pH 7.6, 10% (v/v) glycerol, 150 mM KCl, 0.2 mM EDTA, and 200 μg/ml tRNA. The RNA-bound beads were incubated with 100–250 μg of nuclear extracts in buffer (20 mM HEPES-KOH, pH 7.6, 10% (v/v) glycerol, 150 mM KCl, 0.2 mM EDTA) plus 2.5 mM ATP, 2.0 mM $MgCl_2$, 1000 ng/ml tRNA. Beads were then washed four times with 1 ml of buffer. After the final centrifugation, the proteins bound to the immobilized RNA were eluted in 80 mM Tris-Cl, pH 6.8, 0.1 M dithiothreitol, 2% SDS, 10% glycerol, and 0.2% bromphenol blue for LC-MS/MS and in 1 M Tris, pH 7.0, 10% SDS, 50% glycerol, and 0.1% bromphenol blue for Western analysis by heating for 5 min at 95 °C.

LC-MS/MS and Western Analysis—Proteins eluted from the RNA-linked beads were separated by size in a 10% polyacrylamide gel. The protein bands of interest were visualized by colloidal Coomassie Blue (Invitrogen) and excised from the gels. The gel slices were digested with trypsin (2 μg/ml) overnight at 37 °C. The digests were dried and reconstituted in 5% acetonitrile, 0.1% formic acid and then loaded onto a C_{18} column using a helium pressure cell. Protein peptides were eluted from the column using a linear acetonitrile gradient of 5–50% over 60 min with a flow rate 300 nl/min. The ion trap mass spectrometer (ProteomeX Work station) was programmed to perform a full MS scan followed by MS/MS scans of the five most abundant ions present. Raw data files were compared with the SwissProt data base using SEQUEST software to identify proteins that match the peptide fragments. SEQUEST results were manually confirmed using the criteria described (39). Peptides were accepted if they had a cross-correlation (X_{corr}) score of at least 1.9, 2.2, or 3.7 for the +1, +2, or +3 charge states, respectively. Western analysis was as previously described (40). The hnRNP antibodies (Immuquest) and SR antibodies (Zymed Laboratories Inc.) were purchased from the indicated sources.

RESULTS

The Cis-acting RNA Element Involved in the Inhibition of G6PD Expression in Rat Hepatocytes by Arachidonic Acid Is Located between Nucleotides 43 and 72 of Exon 12—Incubation of primary rat hepatocytes with insulin induces expression of G6PD, whereas the addition of arachidonic acid inhibits G6PD

A

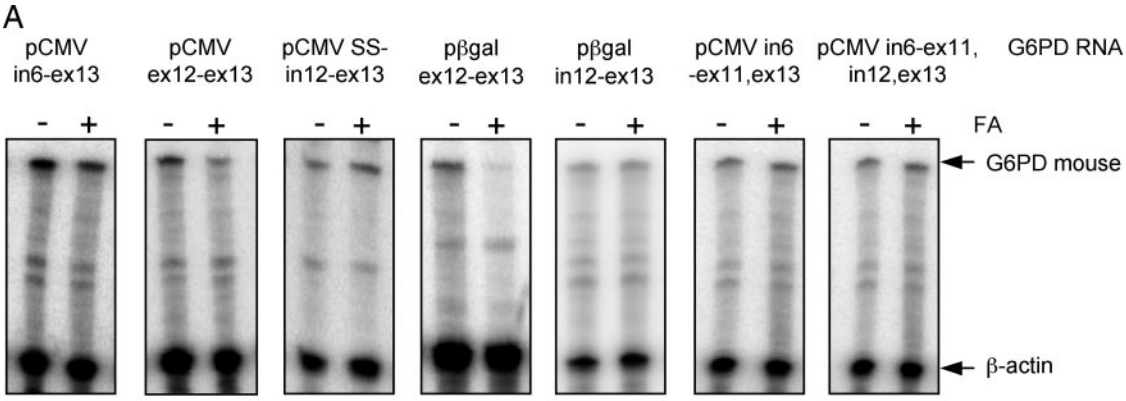

B

Name	G6PD RNA Reporter Constructs	% Inhibition by FA	
		Reporter	Endogenous
pCMV in6-ex13	CMV 7 8 9 10 11 12 13 3'UTR	47 ± 5	56 ± 2
pCMV ex12-ex13	CMV 12 13 3'UTR	49 ± 6	48 ± 3
pCMV SS-in12-ex13	5'-SS CMV 13 3'UTR	9 ± 5	57 ± 2
pβ-gal ex12-ex13	CMV β-galactosidase 12 13 3'UTR	70 ± 9	52 ± 4
pβ-gal in12-ex13	5'-SS CMV β-galactosidase 13 3'UTR	0	51 ± 2
pCMV in6-ex11,ex13	CMV 7 8 9 10 11 13 3'UTR	4 ± 4	40 ± 7
pCMV in6-ex11,in12, ex13	CMV 7 8 9 10 11 13 3'UTR	0, 0	31, 51

FIGURE 1. **The cis-acting element involved in splicing inhibition of G6PD pre-mRNA by arachidonic acid is localized in exon 12.** Primary rat hepatocytes were transfected with the pre-mRNA reporters shown in the figure. Each pre-mRNA reporter contains the CMV promoter to drive its transcription. The *black rectangles* represent exons of the G6PD gene, *striped rectangles* represent the 3′-untranslated region of G6PD, and *gray rectangles* represent the β-galactosidase gene. *SS*, the presence of the 5′ splice site of intron 12 in this construct. After treatment with insulin (0.04 μM) or insulin plus arachidonic acid (175 μM) for 24 h, total RNA was isolated, and reporter and endogenous mRNA were measured using RNase protection assays. *A*, a representative RNase protection assay is shown. *B*, the results are the mean ± S.E. of multiple experiments (separate hepatocyte isolations). The repetition is as follows: $n = 8$ or more experiments for pCMV in6-ex13 and pCMV ex12-ex13; $n = 4$ for pCMV SS-in12-ex13; $n = 3$ for pβgal ex12-13, pβgal in12-ex13, and pCMV in6-ex11,ex13; and $n = 2$ for pCMV in6-ex11,in12,ex13. G6PD and reporter mRNAs were normalized to the amount of β-actin mRNA. The percentage inhibition by arachidonic acid for the pre-mRNA reporters and for the endogenous gene was calculated by dividing the amount of G6PD mRNA in cells treated with insulin and arachidonic acid by the amount in cells treated with insulin alone. *FA*, arachidonic acid.

expression (4). This decrease in G6PD mRNA accumulation is similar to the decrease observed in livers isolated from mice fed a high fat diet (rich in polyunsaturated fatty acids) *versus* in livers isolated from mice fed a low fat diet (3). Regulation of the G6PD gene in intact animals and in primary rat hepatocytes involves a decrease in the efficiency of splicing of G6PD transcripts (2, 6). Because treating rat hepatocytes with arachidonic acid mimics the effect of a high fat diet, we used rat hepatocytes to localize the cis-acting RNA element in the mouse G6PD transcript that is responsible for its splicing regulation. Exon 13 sequences differ between rats and mice. Thus, ribonuclease protection assays using exon 13 riboprobes are able to distinguish between the endogenous rat mRNA and the mRNA produced from a transfected reporter construct that expresses mouse G6PD genomic DNA (6). These transient transfection assays do not use co-transfection to correct for transfection efficiency, because the presence of two viral promoters within the cells increases variability in the data. Instead, the experiments are replicated multiple times to account for differences in transfection efficiency. Furthermore, in our hands, variation in transfection efficiency between treatments (insulin *versus* insulin plus arachidonic acid) is less that 10% (data not shown). In these reporter assays, arachidonic acid inhibited the accumulation of mRNA from G6PD RNA reporters containing exon 12 to a similar extent as the endogenous gene (Fig. 1) (6). Deletion of sequences 5′ of intron 12 abolished the inhibition by arachidonic acid (Fig. 1; pCMV SS-in12-ex13). To confirm that exon 12 contains a regulatory element, we used two approaches. First, exon 12 was deleted from the G6PD reporter construct (pCMV in6-ex11,ex13 and pCMV in6-ex11,in12,ex13). Accumulation of mRNA from these reporter constructs was not inhibited by arachidonic acid, whereas inhibition of the endogenous gene was

observed as expected (Fig. 1). In the second approach, we tested the ability of exon 12 to regulate the accumulation of a heterologous mRNA. The β-galactosidase gene is not regulated by arachidonic acid in rat hepatocytes (data not shown). Sequences from the last 56 nt of exon 12 through the 3′-UTR of the G6PD gene were ligated to the β-galactosidase gene (pβgal ex12-ex13). Accumulation of mRNA from this construct was inhibited by arachidonic acid; however, deletion of exon 12 while maintaining the 5′ splice site of intron 12 (pβgal in12-ex13) eliminates inhibition by arachidonic acid (Fig. 1). Thus, a cis-acting RNA element involved in inhibition of G6PD mRNA accumulation by arachidonic acid is localized in the last 56 nt of exon 12, and this region of exon 12 can regulate expression of a heterologous gene.

To localize the cis-acting element in exon 12, we performed scanning mutagenesis across the exon. 10-nt-long block mutations were made across exon 12 in the context of pre-mRNA reporter pCMV in6-ex13 (Fig. 2*A*, *labeled 1–9*). Exon 12 is 93 nt long. The first two nucleotides at the 5′-end and the last nucleotide at the 3′-end were not mutated so as not to disrupt normal splice site recognition. Each block mutation has the sequence AAGCATGCAA. This sequence does not generate in-frame stop codons, which induce nonsense-mediated decay (41). In addition, we screened this sequence to find ESEs (available on the World Wide Web at exon.cshl.edu/ESE) (42) and ESSs (available on the World Wide Web at genes.mit.edu/fas-ess (19) and cubweb.biology.columbia.edu/pesx (21); it did not have a high score as a known splicing enhancer or silencer. Mutation of sequences between nucleotides 43 and 72 of exon 12 (mutations 5–7) abrogated the inhibition of reporter mRNA accumulation by arachidonic acid (Fig. 2*B*). For all other mutations, the accumulation of mRNA was inhibited to a similar extent as the endogenous G6PD mRNA. In all transfected cells, the amount of endogenous G6PD mRNA was decreased about 40% or more by arachidonic acid (data not shown). Thus, the sequences of nucleotides 1–42 and 73–93 were not required for regulated splicing. To better define the region containing the regulatory sequence, two additional reporter constructs were produced. These RNA reporters contained 15-nt block mutations from nucleotides 33–47 and 67–82 in exon 12. These mutations also abrogated regulation by arachidonic acid, highlighting the regulatory importance of the first and last five nucleotides in the 43–72 regulatory region in exon 12.

Exon 12 Inhibits Splicing of Intron 11 in Vitro and Is Also Able to Inhibit Splicing of Other Introns of G6PD—Our next question concerned the activity of this element. Is it an ESS and/or an ESE? These elements do not have true consensus sequences and can vary both in sequence and length of the element and must be functionally characterized (17, 19, 21, 42). Splicing regulatory sequences have the same activity *in vivo* and *in vitro* (31); thus, we used the *in vitro* splicing assay to define the basal activity of the exon 12 regulatory element. The large amount of ribonucleases in rat hepatocyte nuclear extract (43) precluded its use in the splicing assay. HeLa cell nuclear extract is commonly used for *in vitro* splicing assays and is known to recapitulate splicing activity of various mammalian cell lines (*cf.* Refs. 16 and 31). We compared splicing between three different G6PD *in vitro* splicing substrates: IVS 8-9, IVS 10-11, and IVS 11-12 (Fig. 3*A*). These substrates contain the entire exons and intervening introns present in mouse G6PD RNA. IVS 8-9 and IVS 10-11 were efficiently spliced in HeLa nuclear extract. In contrast, a spliced product for IVS 11-12 was either undetectable or present at less than 5% of the total RNA as compared with the 60–70% rate of splicing for IVS 8-9 or IVS 10-11 (Figs. 3*B* and 4*B*). Splicing of IVS 11-12 was enhanced neither by increasing the incubation time of the assay to 6 h nor by varying the components of the assay (data not shown).

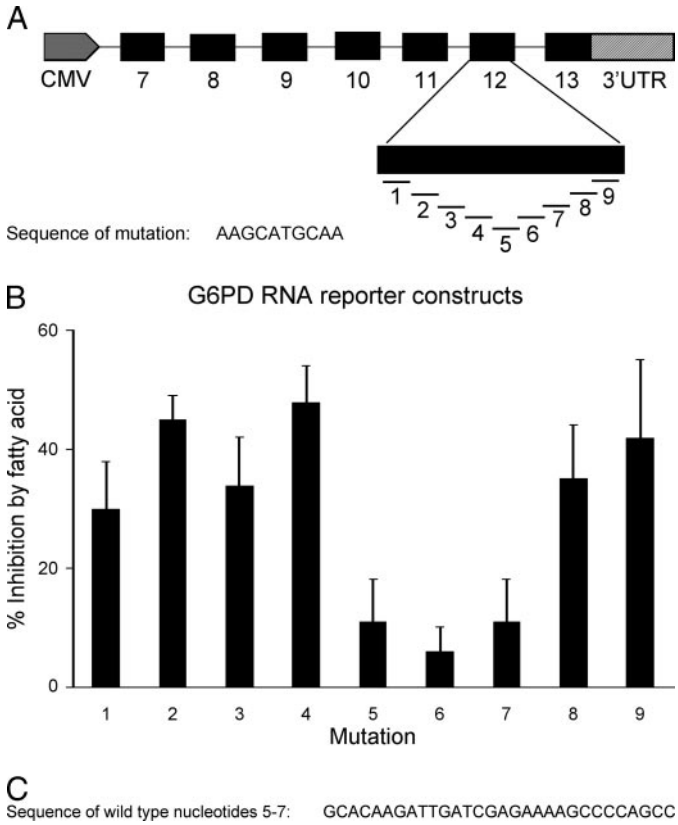

FIGURE 2. **The splicing regulatory element in exon 12 is located between nucleotides 42 and 73.** *A*, structure of the mutated pre-mRNA reporters. *Black rectangles* represent the exons of the G6PD gene, *black lines* represent the introns, and the *gray rectangles* represent the 3′-untranslated region of G6PD. The CMV promoter drove transcription of the reporters. The *lines below exon 12* indicate the mutations. Each mutation contains the indicated sequence in place of the sequence at the following locations: mutation 1, positions 3–12; mutation 2, positions 13–22; mutation 3, positions 23–32; mutation 4, positions 33–42; mutation 5, positions 43–52; mutation 6, positions 53–62; mutation 7, positions 63–72; mutation 8, positions 73–82; mutation 9, positions 83–92. *B*, quantification of reporter G6PD RNA. Transfection, treatment with insulin (0.04 μM) with or without arachidonic acid (175 μM), and RNA assay was as in Fig. 1. The percentage of inhibition by arachidonic acid for the pre-mRNA reporters was calculated by dividing the amount of G6PD mRNA in cells treated with arachidonic acid by the amount in cells not incubated with arachidonic acid. All values were normalized by amount of β-actin mRNA to correct for differences in total RNA amount. Each *bar* shows the mean ± S.E. for at least $n = 3$ separate hepatocyte isolations (mutation 1, $n = 3$; mutations 6 and 7, $n = 4$; mutations 2, 6, and 7, $n = 6$; mutations 3, 5, 8, and 9, $n = 7$; mutation 4, $n = 9$). *C*, sequence of exon 12 from nucleotides 42–73 of the mouse G6PD mRNA.

Several reasons may explain the lack of splicing of IVS 11-12. First, exon 12 *per se* may inhibit splicing *in vitro*. Second, intron 11 may be difficult to splice *in vitro*. Third, the *in vitro* splicing substrate IVS 11-12 may have been constructed in such a way that it could not be spliced. Since IVS 10-11 was efficiently spliced *in vitro*, we ruled out a negative effect of exon 11 on IVS

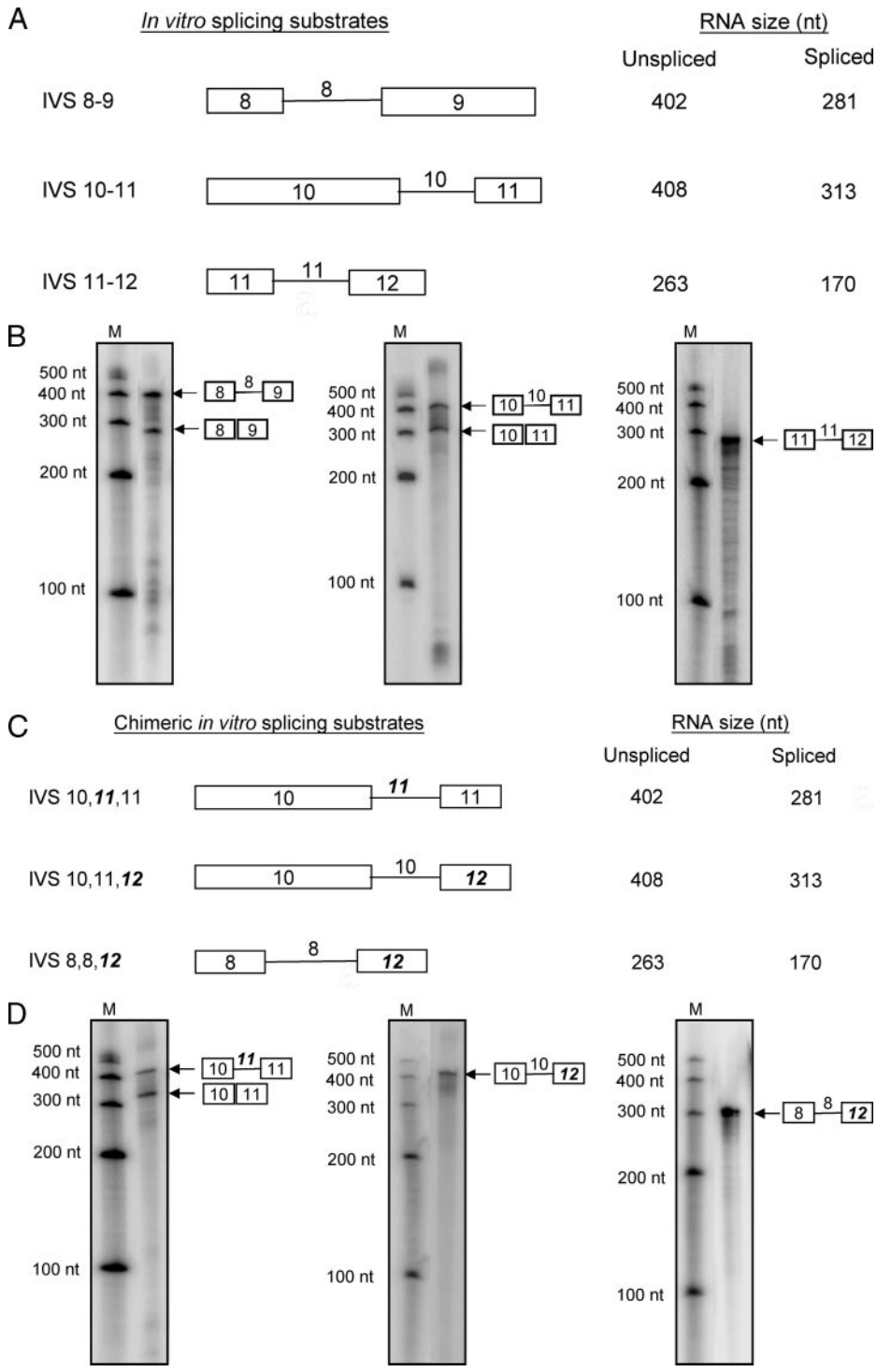

FIGURE 3. **Exon 12 inhibits splicing of different G6PD introns *in vitro*.** *A*, schematic of G6PD *in vitro* splicing substrates with their calculated sizes and the sizes of their spliced products. *Boxes* represent the exons, and *lines* represent the introns of the G6PD gene. *B*, *in vitro* splicing assay. The *in vitro* splicing substrates were incubated in splicing reactions for 60 min, and the substrates and products were resolved by denaturing polyacrylamide gel electrophoresis. The identity of each band is indicated on the *right side* of the gels. Representative gels are shown; repetition was as follows: IVS 8-9 ($n = 15$), IVS 10-11 ($n = 8$), and IVS 11-12 ($n = 12$). *C*, schematic of chimeric splicing substrates containing intron 11 in place of intron 10 in IVS 10,***11***,11, and exon 12 in place of the correct exon in IVS 10,10,***12*** and IVS 8,8,***12***. Exons and introns that were inserted to modify the *in vitro* splicing substrates are shown in *italic boldface type*. *D*, splicing of chimeric substrates in the *in vitro* assay. The splicing substrates and products were resolved with denaturing polyacrylamide gel electrophoresis, and the identity of each band is indicated by the schematic. All splicing reactions were incubated for 240 min. Representative gels are shown; repetition was as follows: IVS 10,***11***,11 ($n = 7$), IVS 10,10,***12*** ($n = 6$), IVS 8,8,***12*** ($n = 4$). In all cases, the molecular weight marker (*M*) was moved closer to the *data lane* for clarity. In two cases, the reactions were run on the same gel, and the *M lane* was reproduced for clarity.

11-12 splicing. To determine if intron 11 or exon 12 are responsible for the absence of splicing of IVS 11-12, we tested splicing of three additional *in vitro* splicing substrates (Fig. 3*C*). In the first substrate (IVS 10,***11***,11), intron 10 was replaced by intron 11 within the context of the efficiently spliced substrate IVS 10-11. IVS 10,***11***,11 was efficiently spliced in the *in vitro* assay (Fig. 3*D*). We next replaced exons 9 and 11 with exon 12 in the context of IVS 8-9 and IVS 10-11, respectively. Splicing was not observed for these chimeric substrates containing exon 12 (Fig. 3*D*). Consistent with the hepatocyte data, exon 12 contains an element that regulates splicing of G6PD pre-mRNA, and in this context the element functions as an ESS inhibiting splicing.

To further confirm that intron 11 does not play a role in the inhibition of splicing of G6PD pre-mRNA, we compared the efficiency of splicing between IVS 8-9, IVS 10-11, and IVS 10,***11***,11 after 30, 60, 120, and 240 min of incubation with HeLa nuclear extract (Fig. 4). For all *in vitro* splicing substrates, spliced products were detected after 30 min of incubation and accumulated with time (Fig. 4, *A* and *B*). The percentage of spliced product generated by IVS 10,***11***,11 was similar to IVS 10-11 at all time points. In contrast, splicing of IVS 8-9 was significantly less at 30 and 60 min ($p < 0.001$) compared with IVS 10-11, indicating that the assay is sensitive enough to detect small changes in spliced product accumulation. The lack of effect of intron 11 on splicing efficiency in the chimeric substrate strengthens our conclusion that exon 12 contains a splicing silencer.

Exon 12 Inhibits Splicing of G6PD Pre-mRNA before the First Catalytic Step—To corroborate the *in vitro* splicing results indicating the presence of an ESS in exon 12, a spliceosome assembly assay was conducted. If the exon 12 regulatory element has a dominant ESS, spliceosome assembly should be inhibited at an early step. The assembly of

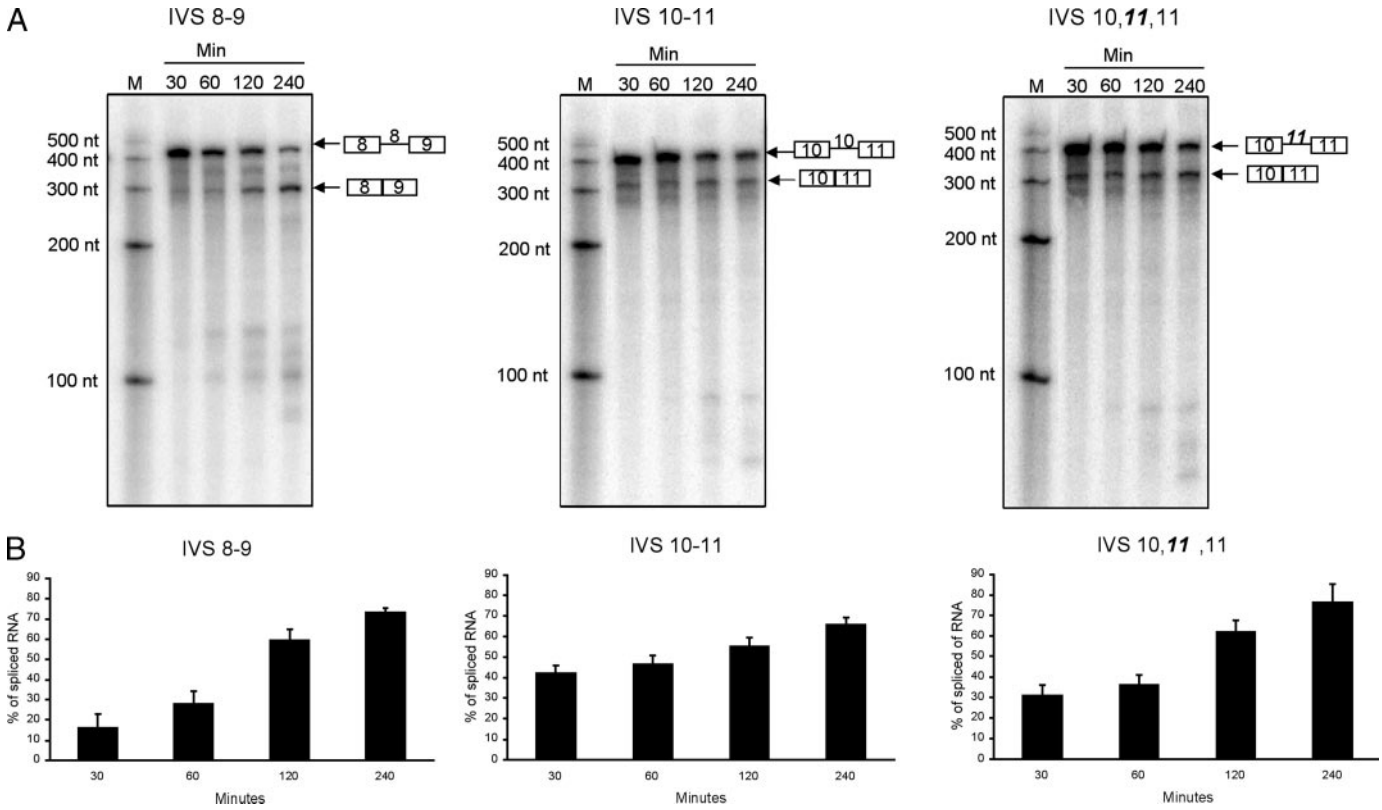

FIGURE 4. **G6PD intron 11 is efficiently spliced in chimeric splicing substrates.** *A*, the splicing substrates IVS 8-9, IVS 10-11, and IVS 10,11,11 described in Fig. 3 were used in *in vitro* splicing assays. The reactions were stopped after 30, 60, 120, and 240 min and resolved on 6% denaturing polyacrylamide gels. *B*, quantification of the splicing efficiency of IVS 8-9, IVS 10-11, IVS 10,11,11 at 30, 60, 120, and 240 min. The splicing products were imaged and quantified using phosphorimaging and ImageQuaNT software. The values are the PhosphorImager units normalized for the C content of the RNA. The percentage of spliced mRNA was calculated as the ratio of the normalized PhosphorImager units of spliced mRNA divided by the sum of the amounts of unspliced plus spliced RNA. Each *bar* represents mean ± S.E. of $n = 3$ experiments for IVS 8-9 and IVS 10,***11***,11 and $n = 5$ experiments for IVS 10-11. The rate of increase of spliced product accumulation for IVS 8-9 is significantly different from IVS 10-11 ($p < 0.001$). Spliced product accumulations between IVS 10-11 and IVS 10,***11***,11 are not significantly different. *M*, marker.

the spliceosome occurs stepwise and is characterized by the interaction of multiple proteins and ribonuclear proteins with the nascent transcript. These RNA and protein complexes are as follows in order of formation: H, E, A, B, and C (15, 34, 44, 45). H is a nonspecific complex formed by interactions of the pre-mRNA with multiple hnRNPs. The composition of this complex can vary greatly in composition between different RNAs but will include splicing regulatory proteins involved in the formation of the catalytically competent spliceosome (46). Its formation occurs even at 0 °C and does not require ATP. Incubation of the pre-mRNA at 30 °C leads to formation of complex E (45). In addition to splicing regulatory proteins, such as the SR proteins and hnRNPs, complex E contains U1 snRNP and the U2AF splicing factors at the 5′ and 3′ splice sites of the intron, respectively (47). Complex A forms following the addition of ATP and involves binding of the splicing factor U2 snRNP to the branch point in the intron (48). Incorporation of the U4/U5/U6 tri-snRNP leads to formation of complex B. Subsequently, after massive structural rearrangements, the catalytically activated spliceosome (complex C) forms, and the first transesterification step of splicing occurs (15).

To determine if spliceosome assembly is inhibited by the ESS present in exon 12, we analyzed the assembly of spliceosome complexes on the splicing substrates. Four different ^{32}P-labeled *in vitro* splicing substrates were used. Three substrates contained G6PD sequences (Fig. 3*A*): IVS 8-9, IVS 10-11 (both are spliced in the *in vitro* splicing assay), and IVS 11-12 (which was not spliced in the *in vitro* splicing assay). The fourth substrate was the human β-globin minigene containing exon 1, intron 1, and exon 2 of human β-globin; it was included as a positive control, because it is robustly spliced (29). In the absence of ATP, only complexes H and E formed on all of the substrates (Fig. 5, *first lane* of each *panel*). Upon the addition of ATP, we observed the formation of complexes A and B + C on β-globin mRNA (Fig. 5, *first panel*). Complexes H + E and B + C did not resolve in 6% polyacrylamide gels. Formation of the A and B + C complexes on the β-globin mRNA was detected as early as 5 min (data not shown). Multiple spliceosome complexes were also formed on the *in vitro* splicing substrates, IVS 8-9 and IVS 10-11; however, accumulation of complexes B + C was not as rapid as in the case of β-globin (Fig. 5, *second* and *third panels*). In contrast, a different pattern of complex formation was observed with IVS 11-12 (Fig. 5, *last panel*). Complexes H + E formed in the absence of ATP, although the mobility of these complexes was faster than with other substrates (Fig. 5, compare the *first lane* of each *panel*). The difference in the mobility of the H + E complexes in IVS 11-12 is not simply due to the smaller size of this splicing substrate (140 nt smaller than IVS 8-9). IVS 8-9 and IVS 10-11 are 100 nt smaller than β-globin, and this did not result in a difference in the mobility of the

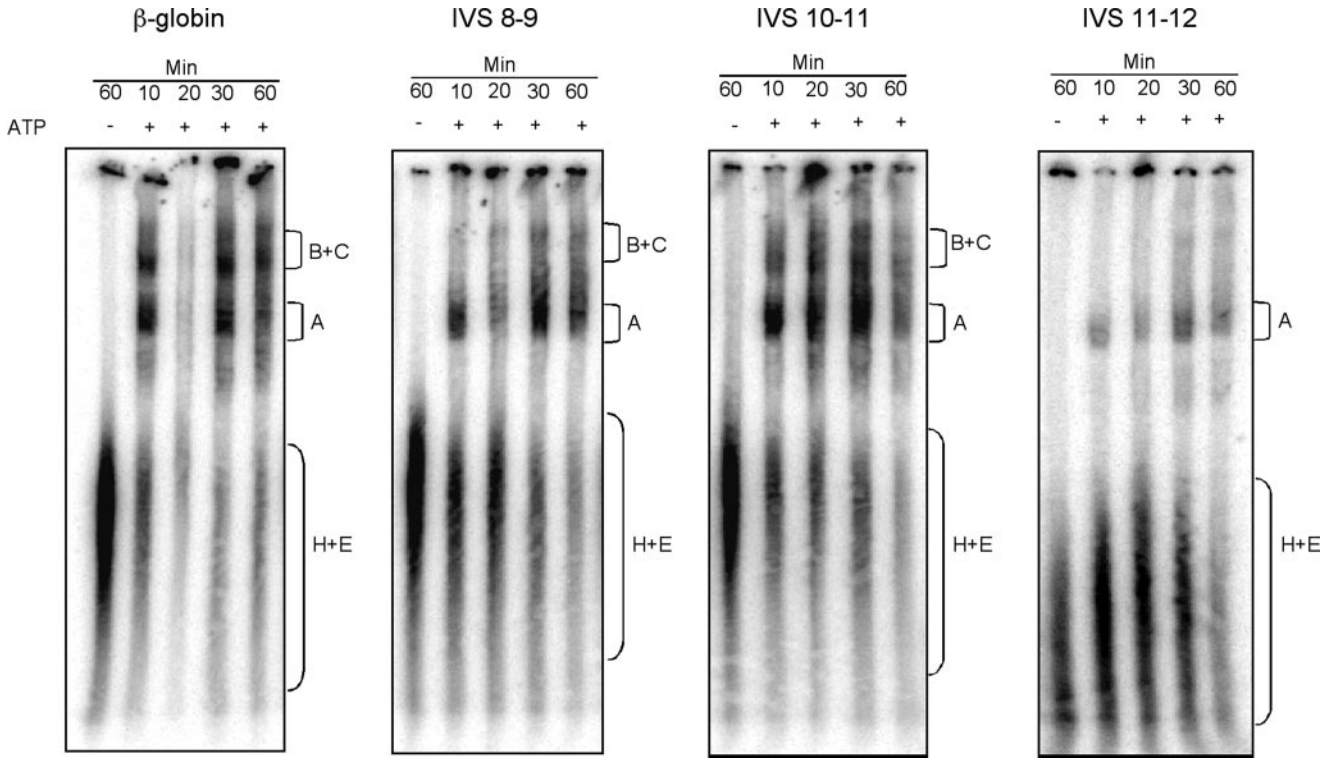

FIGURE 5. **The exon 12 ESS inhibits splicing of IVS 11-12 before the first catalytic reaction.** Four ^{32}P-labeled *in vitro* splicing substrates, β-globin, IVS 8-9, IVS 10-11, and IVS 11-12, were incubated with HeLa cell nuclear extracts under splicing conditions with or without ATP. At the indicated times, aliquots were removed, and the spliceosome complexes were resolved on 4% nondenaturing polyacrylamide gels. The locations of bands corresponding to the spliceosome complexes are indicated on the *right*.

H + E complexes. Upon the addition of ATP, complex A was detected but was much less abundant compared with other splicing substrates. Complexes B + C were not detected at the early time points (10 and 20 min) with little or no accumulation at the later times (30 and 60 min). These results suggest that the ESS present in exon 12 inhibits the assembly of multiple proteins during spliceosome formation.

The altered mobility of complexes H + E and the decrease in formation of complex A on IVS 11-12 suggested that inhibition of splicing may occur at an early step in spliceosome assembly such as assembly of complex E. Because complexes H and E are not resolved in native polyacrylamide gels, we used 1.5% agarose gels to distinguish H and E complexes (35). Complex E was readily detectable with the splicing substrate IVS 11-12 (Fig. 6). Furthermore, the efficiency of complex E formation was similar between IVS 8-9 and IVS 11-12. Thus, complexes H and E formed on IVS 11-12, but the formation of complex A was inhibited. The inhibition of the transition from complex A to B is consistent with the presence of an ESS in the IVS 11-12 RNA substrate.

The Addition of an SC35 Binding Site to IVS 11-12 Can Activate Splicing of Intron 11—If the regulatory sequence is only an ESS, then elimination of this sequence from the RNA should restore splicing. We tested this with two *in vitro* splicing substrates. The first eliminated all sequences 3′ of nucleotide 42 in exon 12 (IVS 11-12 (42)) (Fig. 7*A*). This substrate was not spliced (Fig. 7*B*, *lane 2*). We next eliminated only nucleotides 43–72 of exon 12 (IVS 11-12(Δ43–72)) (Fig. 7*A*). Elimination of just the regulatory region failed to fully restore splicing (Fig. 7*B*, *lane 6*). In some experiments, a faint band, corresponding to the size of the spliced product was observed (*lane 6*, *triangle*). If the element only contained an ESS, its elimination should restore splicing. The fact that it did not could indicate that the regulatory element contains other splicing regulatory sites.

As a second approach to understanding the nature of the exon 12 regulatory element, block mutations that abrogated regulation by arachidonic acid were introduced into the IVS 11-12 splicing substrate. Splicing of the wild type substrate occurred with typical low efficiency (19.3 ± 1%; $n = 3$ experiments). Mutation of nt 43–52 (mutation 5 from Fig. 2) did not alter splicing activity (18.7 ± 4%; $n = 3$). Surprisingly, introduction of mutations 6 (nt 53–62) and 7 (nt 63–72) decreased splicing efficiency by 50%. Splicing activity of IVS 11-12 mutation 6 was 10 ± 2%, and splicing of IVS 11-12 mutation 7 was 9.3 ± 1% ($n = 3$). Although these are very small changes in spliced product formation, they are consistent with the regulatory element having both negative and positive splicing regulatory activity.

ESEs are known to bind splicing co-activators that enhance spliceosome formation by enhancing or stabilizing the interaction of U2 snRNP with the branch point during spliceosome assembly (49). Transition from E complex to A complex requires stable binding of U2 snRNP to the branch point site (50). The decrease in complex A formation observed with IVS 11-12 (Fig. 5) suggests that binding of U2 snRNP to the branch point is either attenuated or less stable compared with the other *in vitro* splicing substrates.

To test if the addition of an SR protein-binding site can induce splicing of IVS 11-12, we ligated an ESE onto exon 12.

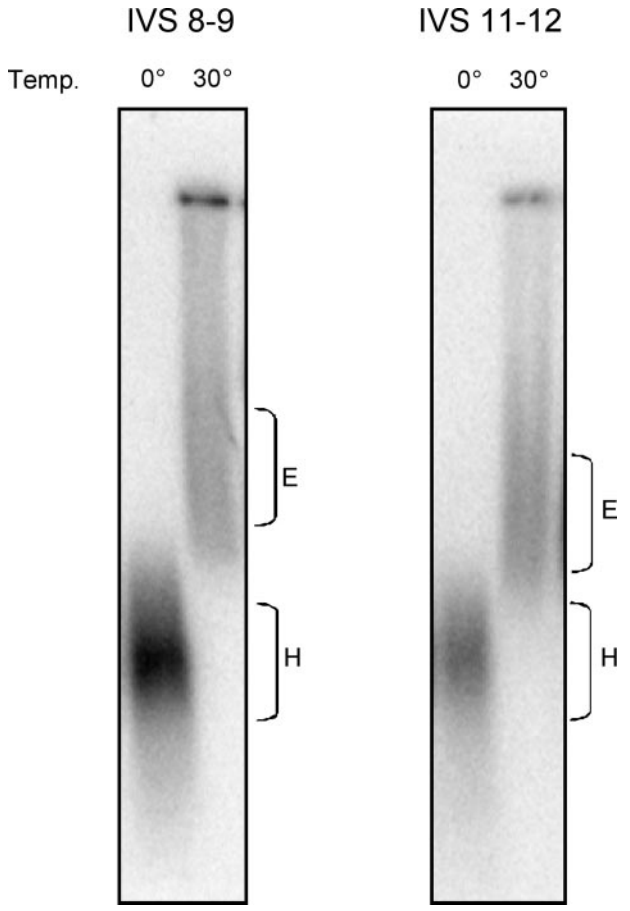

FIGURE 6. **Complex E is efficiently formed on IVS 11-12.** ^{32}P-Labeled RNAs for IVS 8-9 and IVS 11-12 were incubated with HeLa cell nuclear extracts under splicing conditions but in the absence of ATP for 20 min at 0 or 30 °C. Spliceosome assembly was analyzed on 1.5% agarose gels. The locations of complexes H and E are indicated on the *right*.

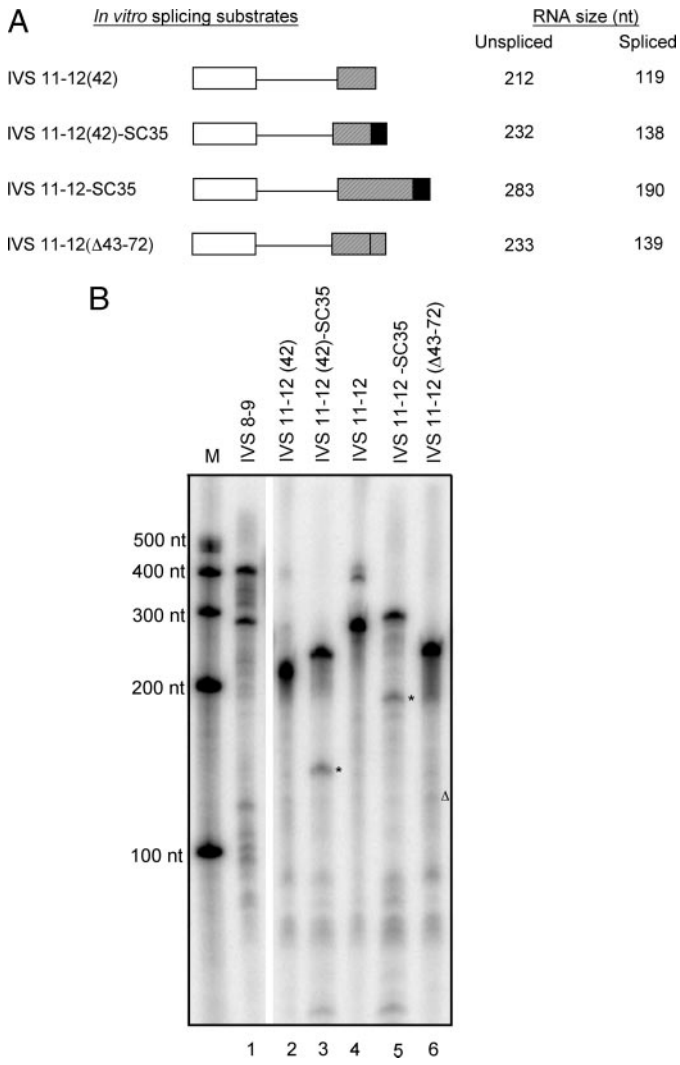

FIGURE 7. **The addition of an SC35 binding site to IVS 11-12 overcomes the inhibitory effect of the exon 12 ESS on splicing of intron 11.** *A*, schematic of modified IVS 11-12 *in vitro* splicing substrates with their calculated sizes and the sizes of their products. *White boxes*, exon 11; *lines between boxes*, intron 11; *gray boxes*, the sequence of exon 12; *black boxes*, nucleotides 50–74 of β-globin exon 2 mRNA (GAUCUGUCCACUCCUGAUGCUGUUA) containing the SC35 binding site (UGCUGUU). *B*, 6% denaturing polyacrylamide gels were used to resolve the substrates and products of the *in vitro* splicing assays. The *asterisk* indicates the spliced products for the substrates: IVS 11-12(42)-SC35 and IVS 11-12-SC35. The *triangle* indicates where a 139-nt spliced product would run for IVS 11-12(Δ43–72). This figure represents a single gel; the *gap* between *lanes 1* and *2* is where lanes were removed from the gel. *M*, marker.

Nucleotides 59–78 of exon 2 of β-globin contain an SC35 binding site (UGCUGUU) (51); this site enhances U2 snRNP binding to the branch point (52). We added this region onto full-length and truncated forms of IVS 11-12 to test if it can induce splicing (IVS 11-12-SC35 and IVS 11-12(42)-SC35, respectively; Fig. 7*A*). The addition of the SC35 binding site induced splicing both in the presence and absence of the ESS (Fig. 7*B*, *lanes 5* and *3*, respectively). Of note, splicing of these substrates was still only 50–60% as efficient as splicing of IVS 8-9, which does not contain an ESS. Thus, the addition of an ESE can overcome the inhibitory effect of the exon 12 ESS. In summary, these data are consistent with the sequence from nucleotides 43–72 of exon 12 containing a dominant ESS and a weak ESE.

Binding of hnRNPs and SR Proteins to the Exon 12 Regulatory Element—ESE sequences bind members of the family of SR proteins and ESS elements are known to bind hnRNPs. An RNA affinity assay was used to determine the proteins that bind to the RNA regulatory element. RNA oligonucleotides were bound to adipic acid beads and incubated with HeLa nuclear extract under splicing conditions. RNA was chemically synthesized to sequences 50–79 (within the regulatory element), 70–93 (outside the regulatory element), and a nonspecific oligomer (containing the sequence of the mutation) (Fig. 2*A*). The oligomer representing the exon 12 regulatory sequences pulled down multiple proteins (Fig. 8*A*). Protein bands at 60 and 37 kDa were specifically detected with RNA representing the regulatory element and not with RNA to other regions of exon 12 (Fig. 8*A*, *lane 1*) or to the nonspecific sequences (Fig. 8*A*, *lane 2*). Bands marked with the *asterisks* were also detected with the adipic acid beads in the absence of bound RNA (data not shown). The band at 45 kDa was not uniformly observed in multiple pull-down experiments. Binding of proteins to the exon 12 regulatory region represented most of the protein binding to the exon as detected using a UV cross-linking assay (Fig. 8*B*). The regions of the gel containing bands at 60 and 37 kDa (band A and B, respectively) were excised and analyzed by LC-MS/MS. Band A contained hnRNPs K, I, and L, and band B

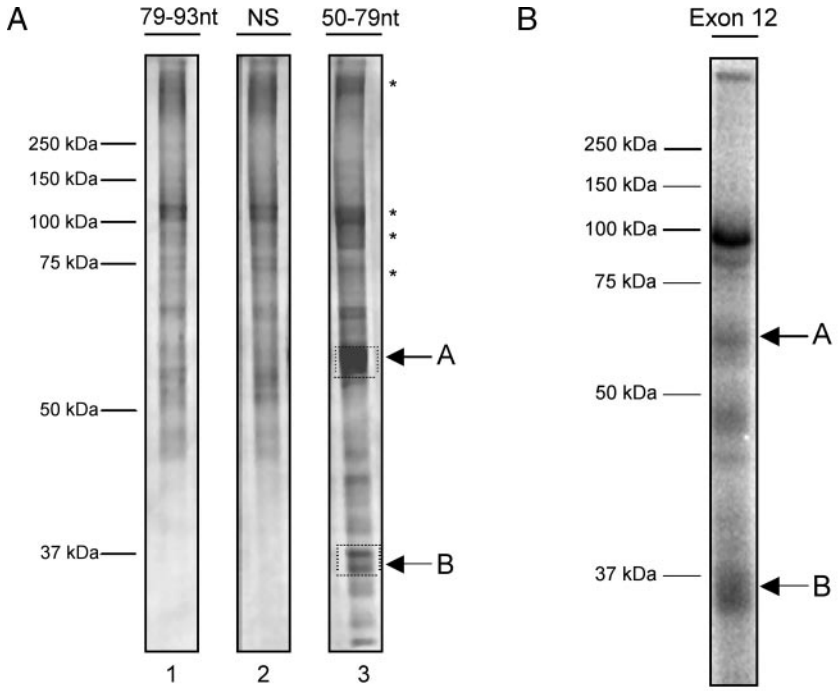

C

	Protein	Protein Accession #	Mass (kDa)	% Sequence covered	Number of Unique Peptides
A	hnRNP K	12230546	50.9	44.3	21
A	hnRNP I	131528	57.1	20.7	6
A	hnRNP L	133274	60.1	10.9	3
B	hnRNP A2/B1	133257	37.4	26.3	8

FIGURE 8. **Identification of proteins binding to exon 12 mRNA by RNA affinity purification.** *A*, RNA oligonucleotides bound to adipic acid beads were mixed with 250 μg of HeLa cell nuclear extract protein. The bound proteins were eluted from the RNA and separated by size on a polyacrylamide gel. The gel was stained with SYPRO Ruby to image the bands and counterstained with colloidal Coomassie Blue to visualize the bands prior to excising for MS/MS analysis. The *boxes* represent the regions excised from the gel. The *asterisks* are bands detected with beads alone. A nonspecific oligonucleotide (*NS*) contained the sequences used in the mutational analysis in Fig. 2 with A residues added to each end to make it 15 nt in length. *B*, exon 12 RNA was *in vitro* transcribed and mixed with 5 μg of HeLa cell nuclear extract protein. UV cross-linking was as described under "Experimental Procedures." The *arrows marked A* and *B* indicate bands of a size corresponding to what was used in MS/MS analysis. *C*, proteins identified by MS/MS analysis in each of the excised bands. The accession numbers correspond to the human data base.

contained hnRNPs A2/B1 (Fig. 8*C*). hnRNPs A2 and B1 are isoforms that differ by only 12 amino acids (53); thus, the specific isoform would not be identified, because the software program used did not search for low scoring peptides ($\Delta C_n > 0.1$; $X_{corr} > 1.9$, 2.2, or 3.7 for the +1, +2, or +3 charge states, respectively).

The binding of these proteins to the exon 12 regulatory element was verified using specific antibodies. These hnRNPs have been demonstrated to regulate RNA processing (10, 17, 37, 46, 54). An oligonucleotide to the full regulatory element (nt 43–72) pulled down hnRNPs K, L, I, and A2/B1 from HeLa cell nuclear extract (Fig. 9*A*, *left panels*). In contrast, these proteins did not bind to sequences outside of the regulatory element (oligonucleotide 79–93; Fig. 9*A*). As a negative control, the blots were probed for hnRNP M, which was not detected in the MS/MS identification. hnRNP M was present in the HeLa nuclear extract but did not bind the nucleotide 43–72 regulatory sequence (Fig. 9*A*). This indicates that this assay detects specific interactions between RNA-binding proteins and their binding sequence.

hnRNPs L, K, and A2/B1 were also present in nuclear extracts from rat hepatocytes (Fig. 9*A*, *right panels*, *input*) and were pulled down by the exon 12 regulatory element (Fig. 9*A*, *right panels*, oligonucleotide 43–72). Little or no binding of these proteins was detected with the sequence from 79 to 93, which is outside the regulatory region. hnRNP A2/B1 did not bind as robustly in the hepatocyte nuclear extract; the reason for this difference is not apparent. In contrast, the hnRNP I amount in hepatocyte nuclear extract was only 5% the amount in HeLa nuclear extract. Thus, little or no hnRNP I was detected binding to the regulatory element in hepatocyte nuclear extract (Fig. 9*A*). The decrease in hnRNP I may reflect tissue-specific differences in the distribution of this protein or a weaker association of this protein with the regulatory element in exon 12. Thus, although it appears to be a binding protein, it may not play a role in regulation of G6PD expression in hepatocytes. Once again, hnRNP M was present in the hepatocyte nuclear extract but did not bind to the regulatory element or the nonregulatory sequence. Thus, hnRNPs L, K, and A2/B1 are exon 12 mRNA-binding proteins in both HeLa cells and primary rat hepatocytes.

The results of the *in vitro* splicing assays (Fig. 7) are consistent with the exon 12 regulatory element also having ESE activity; if this sequence is present, SR proteins should bind to this region. To test for SR protein binding, Western analysis with an antibody to total SR proteins was used against protein affinity-purified by the 43–72 oligonucleotide (Fig. 9*B*). SR proteins of 80, 75, 37 (faint band), and 20 kDa bound to the element in HeLa nuclear extract. No detectable binding was observed with the RNA sequence outside the regulatory region (nt 79–93). In nuclear extracts from rat hepatocytes, only proteins of ~75 kDa

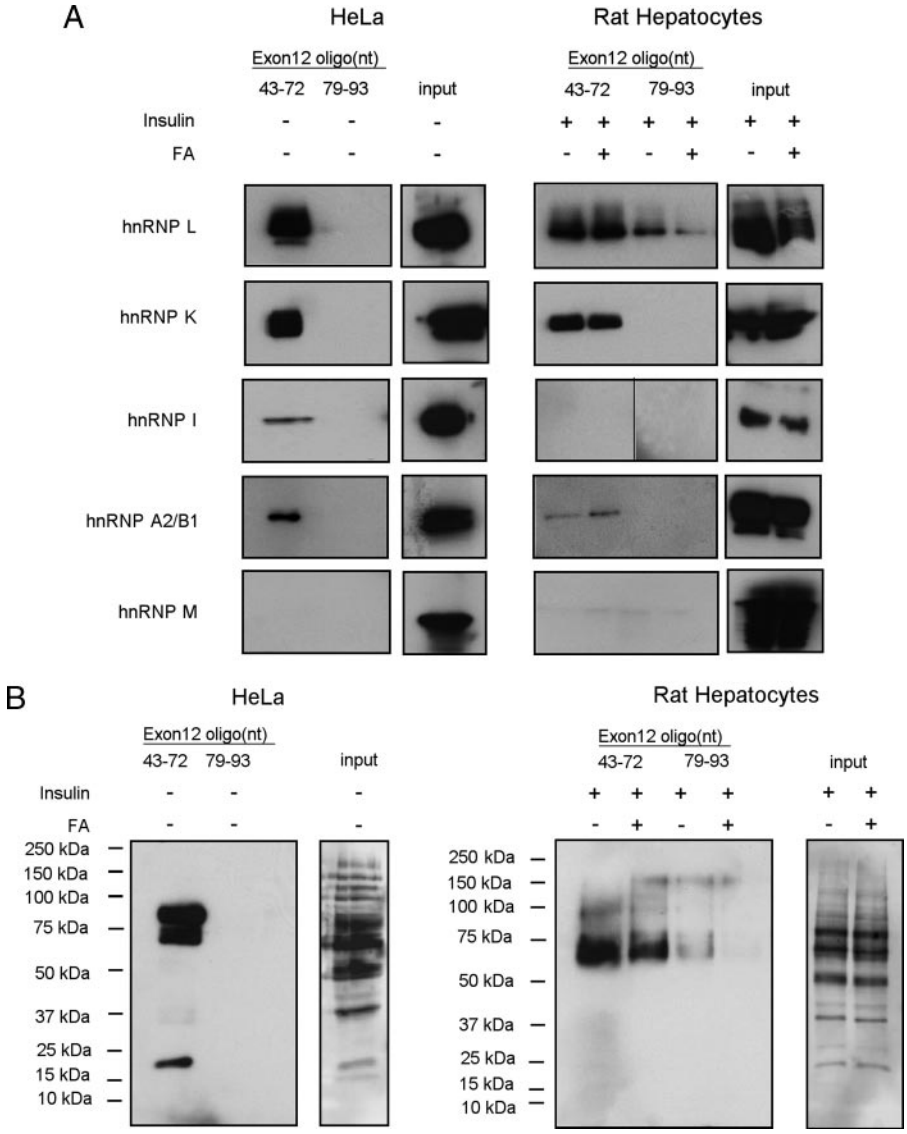

FIGURE 9. **hnRNPs K, L, and A2/B1 and SR proteins in nuclear extracts from HeLa cells and primary rat hepatocytes bind to the exon 12 regulatory element.** Adipic acid beads linked with the indicated RNA oligonucleotides were mixed with 120 μg of HeLa nuclear extract protein and 90 μg of protein from rat hepatocyte nuclear extracts. Rat hepatocytes were incubated with insulin and arachidonic acid as described in Fig. 1. Hepatocytes were harvested for extract preparation after 24 h of treatment. *A*, following elution of the bound proteins with 150 μl of buffer, the amount of eluate analyzed was as follows: 3 μl for detection of hnRNPs K and I, 1 μl for detection of hnRNP L, and 3 μl for hnRNP A2/B1 in HeLa or 10 μl for hnRNP A2/B1 in rat hepatocytes. Input was 2.4 and 3.0 μg of protein for HeLa and hepatocytes, respectively. *B*, for detection of SR proteins, 15 and 20 μl of eluted protein was used for HeLa cells and rat hepatocytes, respectively. These experiments were repeated multiple times with two different nuclear extract preparation; the results of all experiments were similar. *FA*, arachidonic acid.

bound to the element. The absence of SRp20 binding may be due to its lower abundance in rat hepatocyte nuclear extract (Fig. 9*B*; compare inputs). Of note is that considerable more hnRNPs bound to the exon 12 regulatory element than SR proteins. In order to detect SR protein binding to the regulatory element, more protein was loaded onto the gel (*e.g.* for HeLa, 5 times more compared with hnRNP K and A2/B1 and 15 times more than hnRNP L). The amount of protein loaded into the *input lanes* was similar between the hnRNP and SR protein blots, indicating that the proteins are represented in these extracts. The decreased binding of SR proteins to the exon 12 regulatory element is consistent with our splicing data (Fig. 7), indicating that if an ESE is in this regulatory element, it is weaker than the ESS. Alternatively, the ESE and ESS may be juxtaposed to exclude binding of both proteins at the same time.

DISCUSSION

Regulation of G6PD expression is unique. Polyunsaturated fatty acids and nutritional modifications, such as starvation and refeeding, change the accumulation of G6PD mRNA by changes in the rate of pre-mRNA splicing (2, 6). This regulation does not involve changes in the rate of transcription of the gene. In this report, we present evidence that regulation of G6PD splicing by polyunsaturated fatty acid involves an ESS in exon 12 of the G6PD mRNA (Figs. 1 and 2). This element is located between nucleotides 43–72 of exon 12 and can inhibit splicing of heterologous RNAs in intact cells and out of its native context in substrates in the *in vitro* splicing assays (Figs. 2 and 3). This silencer inhibits spliceosome assembly during the formation of complex A (Figs. 5 and 6). Furthermore, the regulatory element is bound by proteins either associated with silencing or with regulation of mRNA processing (Figs. 8 and 9*A*). This is the first report of an RNA element that is involved in the regulation of splicing by arachidonic acid, a polyunsaturated fatty acid, and of the functional characterization of an ESS involved in the regulation of constitutive splicing.

True consensus sequences for ESSs remain to be established. The ESS in exon 12 does not match any known ESSs when screened with available software (19, 21, 42). A similar observation has been made for other ESSs (17). Although we were not able to use nuclear extracts prepared from primary rat hepatocytes for the *in vitro* splicing studies because of the abundance of ribonucleases, the results from *in vitro* splicing assays performed in HeLa cell nuclear extracts are consistent with data obtained from transfection of G6PD pre-mRNA reporters into rat hepatocytes in primary culture (Figs. 1 and 2). Both studies demonstrate a role for this element in inhibiting G6PD splicing.

Few splicing regulatory proteins have been described that function in the inhibition of splicing. The detection of hnRNP L binding to the exon 12 element is consistent with it binding to

the ESS of CD45 mRNA (17). hnRNP A2/B1 inhibits splicing of human immunodeficiency virus RNA and binds an ESS within this viral RNA (55). hnRNP I, also known as polypyrimidine tract-binding protein, also functions in silencing splicing but does so by binding to sequences in introns (10). In contrast, a specific role for hnRNP K in the inhibition of splicing has not been described. This protein appears to play multiple roles in RNA processing, such that it may function *a priori* as a binding partner for other nuclear proteins (54).

Splicing of RNA substrates containing exon 12 was inhibited during complex A formation, which involves the recruitment and stable interaction of U2 snRNP with the branch point in the intron (45). The reduction in complex A formation may be caused by a repressive effect of the exon 12 ESS on the strength of binding of U2 or other splicing factors during the formation of complex A. Activators such as the SR proteins can recruit and or stabilize the interaction of U2 snRNP and thereby the formation of a catalytically active spliceosome (52). The fact that elimination of the exon 12 regulatory region failed to restore robust splicing (IVS 11-12) (42) (Fig. 7), whereas the addition of a strong ESE, capable of binding the ubiquitous SR protein, SC35, restored splicing of this substrate (Fig. 7) is consistent with the need for an ESE in the exon. Juxtaposed ESE and ESS sequences have been described in regulated splicing of a number of mRNAs (23, 24). Our data are consistent with this possibility. In this regard, the 30-nt sequence bound SR proteins that are known to interact with ESE sequences (Fig. 9*B*). The ability of the sequence to bind to both splicing activators, the SR proteins, and inhibitors, hnRNPs, supports the hypothesis of two sequences.

In the *in vitro* splicing assay, the ESS has a dominant inhibitory effect on splicing. In contrast, the abundance of G6PD mRNA is enhanced *in vivo* by insulin and inhibited by arachidonic acid (*e.g.* Fig. 1). Thus, the activity of the regulatory element must also be regulated in response to these treatments. In this regard, arachidonic acid stimulates silencing via this regulatory element, resulting in a decrease in pre-mRNA splicing and thereby a decrease in G6PD mRNA abundance (2, 6) (Fig. 2). In contrast, insulin treatment must enhance splicing potentially via the binding of SR proteins. Insulin has been demonstrated to increase SRp40 phosphorylation and binding to an ESE in the protein kinase CβII mRNA (56). Insulin can also regulate the interaction of hnRNP K with both mRNA and protein binding partners (57). Arachidonic acid inhibits insulin signaling in primary rat hepatocytes, and this inhibition is responsible for the decrease in G6PD mRNA in cells treated with arachidonic acid (40). Therefore, we hypothesize that by attenuating insulin action, arachidonic acid may decrease splicing by decreasing the activity of a splicing activator and thereby facilitating the preferential binding of a splicing inhibitor. Alternatively, insulin and arachidonic acid could more directly regulate the binding and activity of proteins involved in silencing splicing irrespective of SR protein binding. Regulation of G6PD expression by nutritional status is unique to liver and adipose tissue. Furthermore, expression of G6PD in other cell types is very low, consistent with silencing being the default pathway (5). The binding of hnRNPs and SR proteins does not appear to be regulated by arachidonic acid; however, the pull-down approach may be insufficiently sensitive to detect these changes, and/or the posttranslational modifications needed to observe regulated binding might not be maintained in this assay.

More research is still required to finely map the regulatory element to distinguish ESS and ESE sequences and to define the roles of hnRNPs and SR proteins in the regulation of G6PD splicing. The lack of true consensus sequences for both ESEs and ESSs means that these elements must be determined via multiple approaches including functional assays. This work establishes that ESSs can play a role in the splicing of constitutively spliced exons, and this role includes regulation of pre-mRNA splicing in response to nutrient regulation.

Acknowledgments—We are grateful to Dr. Shalini Sharma from the laboratory of Dr. Douglas Black for helpful discussions regarding the spliceosome assembly assay and Dr. Massimo Caputi for assistance with the adipic acid bead protocol. We thank Drs. Kristen Lynch and James Patton for helpful discussions, Dr. William Wonderlin for statistical analysis, Dr. Adrian Krainer for the gift of the β-globin construct, and Dr. Timothy Vincent for help with the LC-MS/MS identifications.

REFERENCES

1. Hillgartner, F. B., Salati, L. M., and Goodridge, A. G. (1995) *Physiol. Rev.* **75,** 47–76
2. Amir-Ahmady, B., and Salati, L. M. (2001) *J. Biol. Chem.* **276,** 10514–10523
3. Stabile, L. P., Hodge, D. L., Klautky, S. A., and Salati, L. M. (1996) *Arch. Biochem. Biophys.* **332,** 269–279
4. Stabile, L. P., Klautky, S. A., Minor, S. M., and Salati, L. M. (1998) *J. Lipid Res.* **39,** 1951–1963
5. Hodge, D. L., and Salati, L. M. (1997) *Arch. Biochem. Biophys.* **348,** 303–312
6. Tao, H., Szeszel-Fedorowicz, W., Amir-Ahmady, B., Gibson, M. A., Stabile, L. P., and Salati, L. M. (2002) *J. Biol. Chem.* **277,** 31270–31278
7. Burmeister, L. A., and Mariash, C. N. (1991) *J. Biol. Chem.* **266,** 22905–22911
8. Siculella, L., Damiano, F., Sabetta, S., and Gnoni, G. V. (2004) *J. Lipid Res.* **45,** 1333–1340
9. Walker, J. D., Burmeister, L. A., Mariash, A., Bosman, J. F., Harmon, J., and Mariash, C. N. (1996) *Endocrinology* **137,** 2293–2299
10. Black, D. L. (2003) *Annu. Rev. Biochem.* **72,** 291–336
11. Berget, S. M. (1995) *J. Biol. Chem.* **270,** 2411–2414
12. Liu, H. X., Zhang, M., and Krainer, A. R. (1998) *Genes Dev.* **12,** 1998–2012
13. Tacke, R., and Manley, J. L. (1995) *EMBO J.* **14,** 3540–3551
14. Blencowe, B. J. (2000) *Trends Biochem. Sci.* **25,** 106–110
15. Hertel, K. J., and Graveley, B. R. (2005) *Trends Biochem. Sci.* **30,** 115–118
16. Caputi, M., and Zahler, A. M. (2002) *EMBO J.* **21,** 845–855
17. Rothrock, C. R., House, A. E., and Lynch, K. W. (2005) *EMBO J.* **24,** 2792–2802
18. Staffa, A., and Cochrane, A. (1995) *Mol. Cell. Biol.* **15,** 4597–4605
19. Wang, Z., Rolish, M. E., Yeo, G., Tung, V., Mawson, M., and Burge, C. B. (2004) *Cell* **119,** 831–845
20. Grabowski, P. J. (2004) *Biochem. Soc. Trans.* **32,** 924–927
21. Zhang, X. H., and Chasin, L. A. (2004) *Genes Dev.* **18,** 1241–1250
22. Tong, A., Nguyen, J., and Lynch, K. W. (2005) *J. Biol. Chem.* **280,** 38297–38304
23. Zahler, A. M., Damgaard, C. K., Kjems, J., and Caputi, M. (2004) *J. Biol. Chem.* **279,** 10077–10084
24. Zhu, J., Mayeda, A., and Krainer, A. R. (2001) *Mol. Cell* **8,** 1351–1361
25. Seglen, P. O. (1973) *Exp. Cell Res.* **82,** 391–398
26. Shih, H. M., and Towle, H. C. (1995) *BioTechniques* **18,** 813–814, 816

27. Mooney, R. A., and Lane, M. D. (1981) *J. Biol. Chem.* **256,** 11724–11733
28. Horton, R. M., Cai, Z. L., Ho, S. N., and Pease, L. R. (1990) *BioTechniques* **8,** 528–535
29. Lopato, S., Mayeda, A., Krainer, A. R., and Barta, A. (1996) *Proc. Natl. Acad. Sci. U. S. A.* **93,** 3074–3079
30. Chomczynski, P., and Sacchi, N. (1987) *Anal. Biochem.* **162,** 156–159
31. Mayeda, A., and Krainer, A. R. (1999) *Methods Mol. Biol.* **118,** 309–314
32. Mayeda, A., and Krainer, A. R. (1999) *Methods Mol. Biol.* **118,** 315–321
33. Snedecor, G. W., and Cochran, W. G. (1967) *Statistical Methods*, 6th Ed., Iowa State University Press, Ames, IA
34. Konarska, M. M., and Sharp, P. A. (1987) *Cell* **49,** 763–774
35. Reed, R., and Chiara, M. D. (1999) *Methods* **18,** 3–12
36. Edwalds-Gilbert, G., and Milcarek, C. (1995) *Mol. Cell. Biol.* **15,** 6420–6429
37. Caputi, M., Mayeda, A., Krainer, A. R., and Zahler, A. M. (1999) *EMBO J.* **18,** 4060–4067
38. Langland, J. O., Pettiford, S. M., and Jacobs, B. L. (1995) *Protein Expression Purif.* **6,** 25–32
39. Link, A. J., Eng, J., Schieltz, D. M., Carmack, E., Mize, G. J., Morris, D. R., Garvik, B. M., and Yates, J. R., III (1999) *Nat. Biotechnol.* **17,** 676–682
40. Talukdar, I., Szeszel-Fedorowicz, W., and Salati, L. M. (2005) *J. Biol. Chem.* **280,** 40660–40667
41. Maquat, L. E. (2004) *Nat. Rev. Mol. Cell. Biol.* **5,** 89–99
42. Cartegni, L., Wang, J., Zhu, Z., Zhang, M. Q., and Krainer, A. R. (2003) *Nucleic Acids Res.* **31,** 3568–3571
43. Mayeda, A., Screaton, G. R., Chandler, S. D., Fu, X. D., and Krainer, A. R. (1999) *Mol. Cell. Biol.* **19,** 1853–1863
44. Gozani, O., Patton, J. G., and Reed, R. (1994) *EMBO J.* **13,** 3356–3367
45. Michaud, S., and Reed, R. (1991) *Genes Dev.* **5,** 2534–2546
46. Dreyfuss, G., Matunis, M. J., Pinol-Roma, S., and Burd, C. G. (1993) *Annu. Rev. Biochem.* **62,** 289–321
47. Staknis, D., and Reed, R. (1994) *Mol. Cell. Biol.* **14,** 2994–3005
48. Query, C. C., McCaw, P. S., and Sharp, P. A. (1997) *Mol. Cell. Biol.* **17,** 2944–2953
49. Furuyama, S., and Bruzik, J. P. (2002) *Mol. Cell. Biol.* **22,** 5337–5346
50. Das, R., Zhou, Z., and Reed, R. (2000) *Mol. Cell* **5,** 779–787
51. Schaal, T. D., and Maniatis, T. (1999) *Mol. Cell. Biol.* **19,** 261–273
52. Fu, X. D., and Maniatis, T. (1992) *Proc. Natl. Acad. Sci. U. S. A.* **89,** 1725–1729
53. Kamma, H., Satoh, H., Matusi, M., Wu, W. W., Fujiwara, M., and Horiguchi, H. (2001) *Immunol. Lett.* **76,** 49–54
54. Bomsztyk, K., Denisenko, O., and Ostrowski, J. (2004) *BioEssays* **26,** 629–638
55. Bilodeau, P. S., Domsic, J. K., Mayeda, A., Krainer, A. R., and Stoltzfus, C. M. (2001) *J. Virol.* **75,** 8487–8497
56. Patel, N. A., Kaneko, S., Apostolatos, H. S., Bae, S. S., Watson, J. E., Davidowitz, K., Chappell, D. S., Birnbaum, M. J., Cheng, J. Q., and Cooper, D. R. (2005) *J. Biol. Chem.* **280,** 14302–14309
57. Ostrowski, J., Kawata, Y., Schullery, D. S., Denisenko, O. N., Higaki, Y., Abrass, C. K., and Bomsztyk, K. (2001) *Proc. Natl. Acad. Sci. U. S. A.* **98,** 9044–9049